



Ras-Induced miR-146a and 193a Target *Jmjd6* to Regulate Melanoma Progression

Viviana Anelli¹, Anita Ordas², Susanne Kneitz³, Leonel Munoz Sagredo^{4,5}, Victor Gourain⁴, Manfred Schartl^{3,6,7}, Annemarie H. Meijer² and Marina Mione^{1*}

¹ Cibio, University of Trento, Trento, Italy, ² Institute of Biology, Leiden University, Leiden, Netherlands, ³ Physiological Chemistry, Biocenter, University of Würzburg, Würzburg, Germany, ⁴ Institute of Toxicology and Genetics, Karlsruhe Institute of Technology, Karlsruhe, Germany, ⁵ Faculty of Medicine, University of Valparaíso, Valparaíso, Chile, ⁶ Comprehensive Cancer Center, University Clinic Würzburg, Würzburg, Germany, ⁷ Hagler Institute for Advanced Study and Department of Biology, Texas A&M University, College Station, TX, United States

OPEN ACCESS

Edited by:

Maria Grazia Giansanti,
Consiglio Nazionale delle Ricerche
(CNR), Italy

Reviewed by:

Victoriano Mulero,
University of Murcia, Spain
Theodora Katsila,
University of Patras, Greece

*Correspondence:

Marina Mione
mariacaterina.mione@unitn.it

Specialty section:

This article was submitted to
Genetic Disorders,
a section of the journal
Frontiers in Genetics

Received: 28 September 2018

Accepted: 04 December 2018

Published: 18 December 2018

Citation:

Anelli V, Ordas A, Kneitz S,
Sagredo LM, Gourain V, Schartl M,
Meijer AH and Mione M (2018)
Ras-Induced miR-146a and 193a
Target *Jmjd6* to Regulate Melanoma
Progression. *Front. Genet.* 9:675.
doi: 10.3389/fgene.2018.00675

Ras genes are among the most commonly mutated genes in human cancer; yet our understanding of their oncogenic activity at the molecular mechanistic level is incomplete. To identify downstream events that mediate ras-induced cellular transformation *in vivo*, we analyzed global microRNA expression in three different models of Ras-induction and tumor formation in zebrafish. Six microRNAs were found increased in Ras-induced melanoma, glioma and in an inducible model of ubiquitous Ras expression. The upregulation of the microRNAs depended on the activation of the ERK and AKT pathways and to a lesser extent, on mTOR signaling. Two Ras-induced microRNAs (miR-146a and 193a) target *Jmjd6*, inducing downregulation of its mRNA and protein levels at the onset of Ras expression during melanoma development. However, at later stages of melanoma progression, *jmjd6* levels were found elevated. The dynamic of *Jmjd6* levels during progression of melanoma in the zebrafish model suggests that upregulation of the microRNAs targeting *Jmjd6* may be part of an anti-cancer response. Indeed, triple transgenic fish engineered to express a microRNA-resistant *Jmjd6* from the onset of melanoma have increased tumor burden, higher infiltration of leukocytes and shorter melanoma-free survival. Increased *JMJD6* expression is found in several human cancers, including melanoma, suggesting that the up-regulation of *Jmjd6* is a critical event in tumor progression.

The following link has been created to allow review of record GSE37015: <http://www.ncbi.nlm.nih.gov/geo/query/acc.cgi?token=jjcrbiuicyyqgpc&acc=GSE37015>.

Keywords: zebrafish, cancer models, microRNA, *Jmjd6*, ras, melanoma, miR-146a, miR-193a

INTRODUCTION

Activating mutations in the RAS genes or in other members of the ras-signaling pathways are very common in cancer¹ and recent deep sequencing data of cancer genomes² suggest that these mutations are important primers of malignancies. Still, the initial molecular events following activation of the pathways downstream of Ras are extremely difficult to study *in vivo*.

¹<http://www.sanger.ac.uk/genetics/CGP/cosmic/>

²<http://cancergenome.nih.gov/>

Transgenic models, where the expression of the oncogene leads to cancer development in a reproducible manner provide a suitable experimental system for addressing the complexity of cellular transformation in live animals. The oncogenic versions of the human RAS genes (KRAS, HRAS, and NRAS) have been the first and most successful drivers of cancer in transgenic mice (Chin et al., 1999a,b; Johnson et al., 2001; Malumbres and Barbacid, 2003). This ability of ras oncogenes to initiate and maintain cancer has been related to global molecular and epigenetic changes at early stages of transformation. Among the targets of oncogenes, microRNAs are well-suited to sustain global changes of cellular functions. Changes in several protein levels may be regulated by a single or just a few microRNAs and a number of microRNAs have been found deregulated in cancer (Harrandah et al., 2018). Yet, very few studies have investigated their roles at the onset of transformation as possible “global effectors” of oncogenesis. In this study we have investigated the link between Ras-induced transformation and microRNA expression, using genetically tractable zebrafish models where the expression of a constitutively active *HRAS*^{G12V} allele leads to the development of different cancer types. We found that activated Ras signaling promotes the rapid increase of six microRNAs. Interestingly, two of these microRNAs target the same gene, *Jmjd6*, a jumonjiC domain protein with at least two reported functions: histone arginine demethylation (Chang et al., 2007) and mRNA splicing regulation (Webby et al., 2009). Results reported here indicate that *Jmjd6* is a critical player in zebrafish melanoma development and that at least two Ras-induced microRNAs antagonize *Jmjd6* activation.

RESULTS

Dynamic Regulation of MicroRNAs by RAS Activation

To identify miRNAs that are regulated by oncogenic Ras from the earliest stages of transformation, we used a custom Agilent microarray (see M&M). We profiled miRNA expression in transgenic zebrafish overexpressing *HRAS*^{G12V} in melanocytes (Santoriello et al., 2010), in brain cells (Mayrhofer et al., 2017) and ubiquitously (Santoriello et al., 2009) (**Figure 1A**). Six miRNAs (miR-21.1, miR-21.2, miR-146a, miR-146b-1, miR-193a, miR-193a-1) were up-regulated ($\log_2FC > 1.2$ and $p\text{-value} < 0.01$, see **Supplementary Table S1**) in all three transgenic models at 3 day post-fertilization (dpf) and in 7 dpf melanoma, whereas no commonly down-regulated miRNAs were found (**Figure 1B** and **Supplementary Table S1**, highlighted rows).

This study, we focused on the melanoma model, and to clarify the potential roles of the upregulated microRNAs in melanoma progression, we analyzed microRNA expression levels at four time points (3, 7, and 14 dpf and in adult tumors, **Supplementary Table S1**) during melanoma progression. Next, we designed Taqman probes for the active strand (−5p) of miR21, miR-146a and miR-146b and for the active strand (−3p) of miR-193a and validated the expression levels of the six upregulated miRNAs by qPCR in the melanoma model (**Figure 1C**). The expression of the six microRNA genes showed dynamic patterns: one was

upregulated up to 7 dpf (miR-146b-1-5p), while the others were upregulated to different extents up to adult melanoma (**Figure 1D** and **Supplementary Table S1**). To further validate the dependence of these microRNAs on ras we used drugs that target different pathways downstream of ras. Next, expression levels of miR-21-5p (including both mir21-1 and miR21-2), miR-146a-5p, miR-146b-1-5p, and miR-193a-3p (including also mir193a-1-3p) were quantified through qPCR, after induction of ras expression and in the presence of drugs. For simplicity, the microRNAs under study are named miR-21, miR-146a, miR-146b, miR-193a from now on.

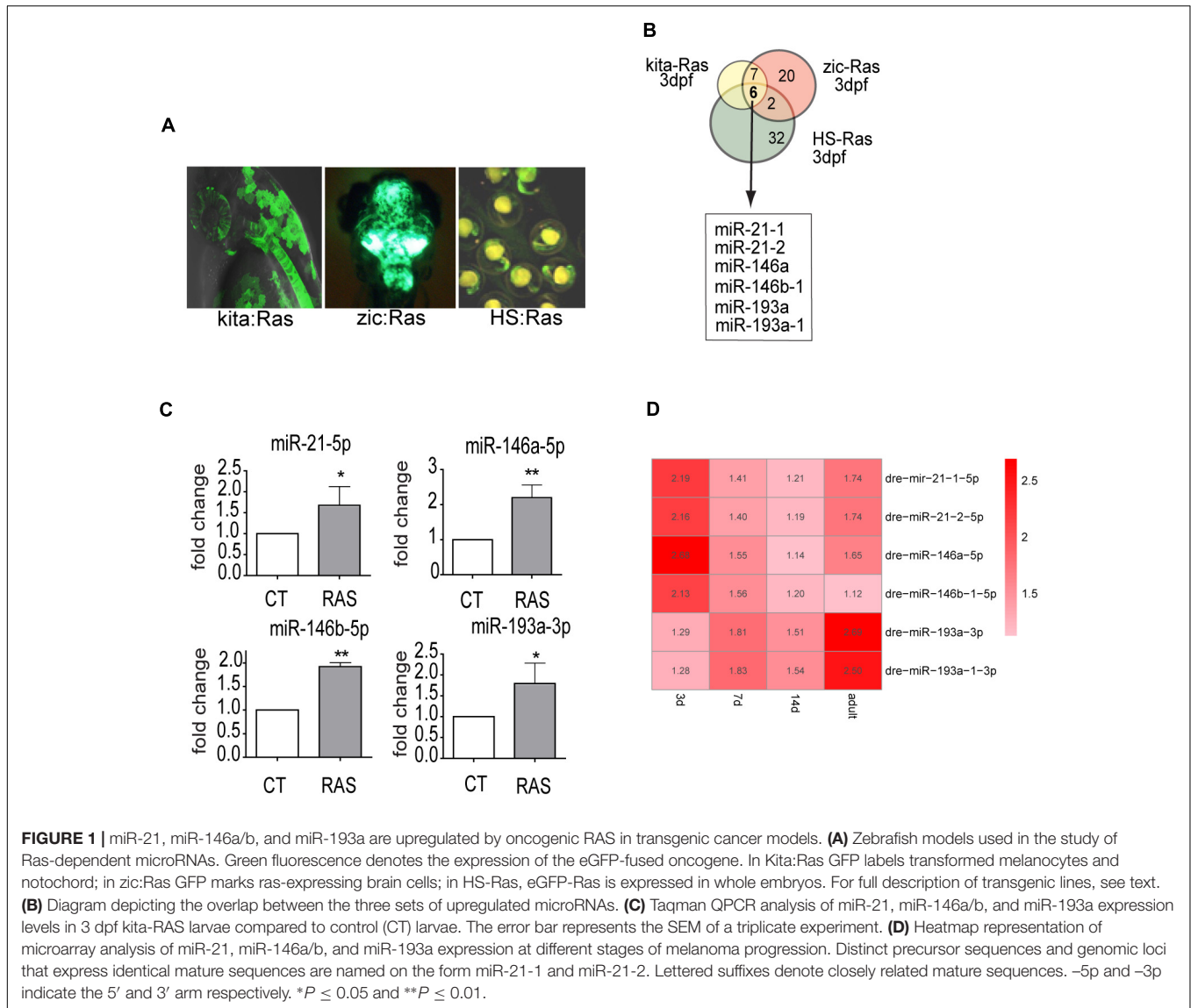
The Increase of miR-21, miR-146a, and miR-193a Is Ras-Dependent

To investigate whether miR-21, miR-146a, miR-146b, and miR-193a are direct targets of ras, we analyzed their expression profiles using an inducible model, *Tg(hsp70l:EGFP-HRASV12)*^{io3}, called HS-RAS, that expresses oncogenic ras upon heat shock. RNA was extracted from 3 dpf HS-RAS embryos, 6 h after a 30 min heat shock treatment at 37°C, when robust ras activation occurs (Santoriello et al., 2009). QPCR data show that miR-21 and miR-146a are significantly upregulated in Ras overexpressing larvae (**Figure 2A**), thus supporting the hypothesis that miR-21 and miR-146a represents early-response targets, likely to be directly induced by oncogenic Ras. MiR-193a and miR-146b did not show significant upregulation in response to ras; however, we performed the inhibitor experiments also on these two microRNAs as they had shown to be upregulated in the melanoma model (**Figure 1C**).

To identify which signaling pathway(s) downstream of Ras induces overexpression of these microRNAs, we blocked specific pathways in HS-RAS larvae using small chemical inhibitors of ERK, AKT and mTOR phosphorylation (**Figure 2B**). To check the efficacy of the inhibitors, we collected treated larvae at 3 dpf and performed western blot analysis for known targets of the three inhibitors. As shown in **Figure 2C** PD98059, rapamycin and LY29004 were able to decrease ERK-P, AKT-P and S6-P levels, respectively. Next we checked the levels of microRNAs in inhibitor treated larvae using qPCR. As shown in **Figures 2D,E**, induction of miR-21 and -146a expression was greatly attenuated by all three inhibitors and most robustly by the ERK inhibitor. MiR-146b levels were not affected by the drug treatments (**Figure 2F**) and miR-193a levels were reduced to statistically significant levels only when larvae were treated with rapamycin (**Figure 2G**). These data suggest that miR-21, miR-146a and to a less extent, miR-193a, are ras-responsive genes and their activation is regulated mostly by the MAPK/ERK and mTOR (for miR-193a) branches of ras signaling.

Predicted Target of MicroRNAs 146a and 193a

As the function of miR-21 is widely studied in cancer (Frezzetti et al., 2011), and miR-146b was found not to respond to Ras signaling, in this study we focused on miR-146a and -193a, to clarify whether they have a role in melanomagenesis.



A web-based target prediction algorithm [MicroCosmTargets, now incorporated in www.tools4mirs.org (Lukasik et al., 2016)], was used to identify potential targets of zebrafish miR-146a and miR-193a. The tool is based on the genome assembly ZV³ and returned a few targets that were selected to contain seed sequences for miR-146a, miR-193a or both, this last category included only *jmjd6*. We then used a web-based interaction-prediction algorithm for RNA molecules, IntaRNA⁴ (Mann et al., 2017) for the fast and accurate prediction of interactions between miR-146a and/or 193a with *jmjd6* mRNAs using the newest genome assembly, GRCz11⁵. This search confirmed the presence of seed sequences for miR-146a and -193a (see **Supplementary Figures S1A,B**).

³http://mar2015.archive.ensembl.org/Danio_rerio/Info/Index

⁴<http://rna.informatik.uni-freiburg.de/IntaRNA/Input.jsp>

⁵https://www.ensembl.org/Danio_rerio/Info/Index

Jmjd6 Is a Target of miR-193a and miR-146a

Danio rerio jmjd6 has 1 transcript (Ensemble, ENSDAR G00000102896). The 3' UTR region of *Jmjd6* contains miRNA recognition elements (MREs) for miR-146a (**Supplementary Figure S1A**), and MREs for miR-193a (**Supplementary Figure S1B**). To determine whether *Jmjd6* is a bona fide target of miR-193a and miR-146a, we tested whether miR-193a and miR-146a expression affects *jmjd6* levels using an *in vivo* GFP reporter assay. The entire *jmjd6*-3' UTR was cloned downstream of green fluorescent protein (GFP) open reading frame (**Figure 3A**). *In vitro* synthesized mRNA from this construct was then injected into single-cell zebrafish embryos with or without miR-193a or miR-146a duplexes (**Figure 3A**), which mimic microRNA overexpression. The injection of the microRNA duplexes resulted in increased levels of microRNA (**Supplementary Figure S2A**) and caused mild

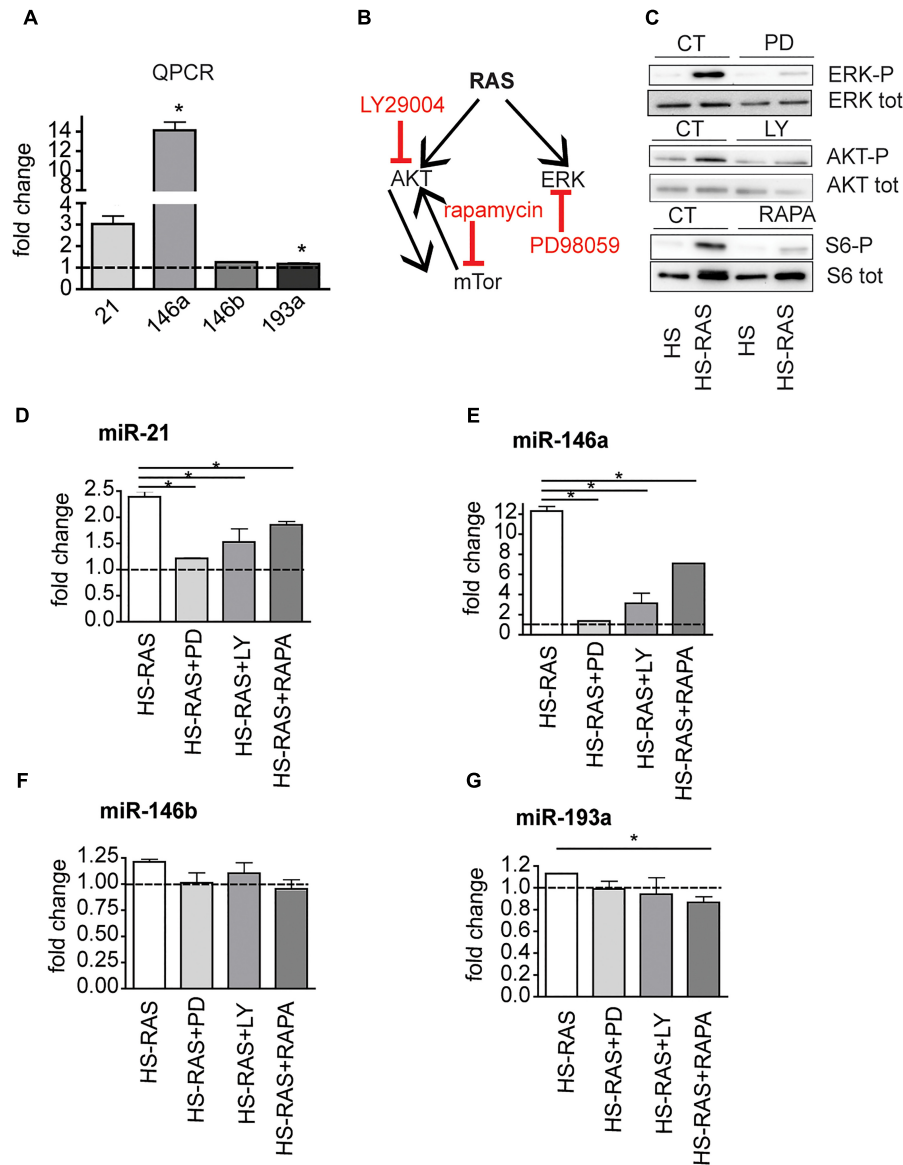


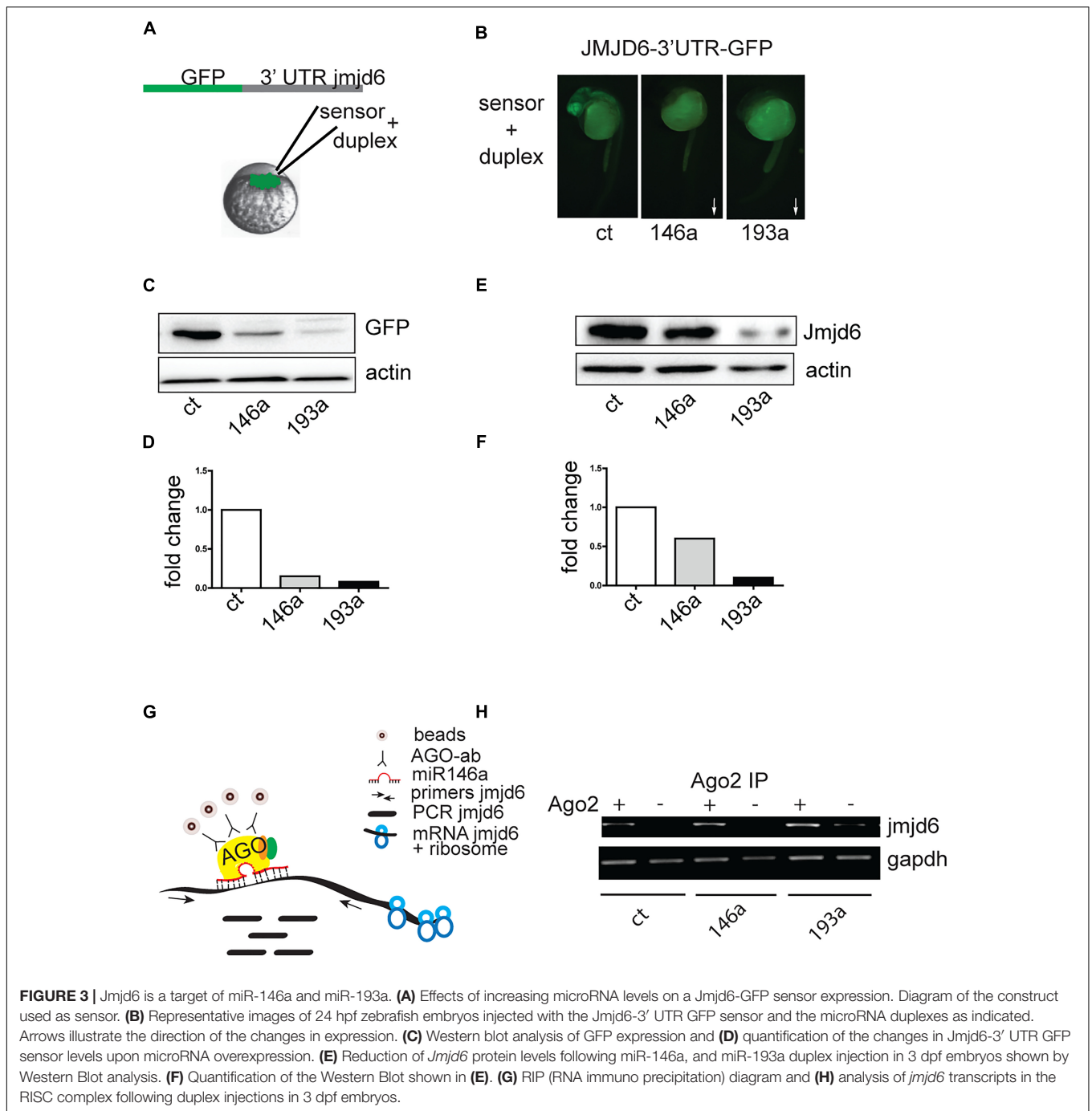
FIGURE 2 | The increase of miR-21, miR-146a/b, and miR-193a is RAS-dependent. **(A)** Taqman QPCR analysis of miR-21, 146a, 146b, and 193a expression following ras upregulation (6 h after heat-shock induction), * $p < 0.05$. **(B)** Diagram showing the ras pathway inhibitors used and their targets. **(C)** Western Blot analysis of ERK-P, AKT-P, and S6-P ribosomal protein levels after the inhibitors treatment. **(D–G)** Taqman qPCR analysis in 3 dpf HS-RAS zebrafish treated with PD98059, LY29004 and rapamycin. The error bars represent the SEM of a triplicate experiment; two tailed Student's test was used for analysis. * $p < 0.05$.

or no phenotypes (**Supplementary Figure S2B**). The following day, GFP expression levels were monitored by fluorescence microscopy (**Figure 3B**) and by western blot analysis with an antibody against GFP (**Figures 3C,D**). In both assays, GFP levels were reduced in embryos injected with miR-193a or miR-146a duplexes. Duplex injection of either miR-146a or miR-193a also resulted in reduction of Jmjd6 protein levels (**Figures 3E,F**).

To validate the direct interaction between miR-146a and miR-193a with *jmjd6* mRNA, we performed RNA immunoprecipitation (RIP, **Figure 3G**). After immunoprecipitation (IP) with Ago2 antibody, which selectively

enriched for RISC complex components (Ikeda et al., 2006), *jmjd6* transcripts were readily found in embryos injected with miR-146a and miR-193a duplexes (**Figure 3H**) suggesting that a physical interaction between *jmjd6* transcripts and specific microRNAs occurs in the RISC complex. These data confirmed the interaction between miR-146a and miR-193a with *jmjd6* mRNA.

As we found that *jmjd6* is a target of miR-146a and -193a, we investigated whether the level of *jmjd6* was lower in Ras expressing larvae compared to controls. As shown in **Supplementary Figures S3A,B** heat-shock induced Ras overexpression results in down-regulation of *jmjd6* RNA level

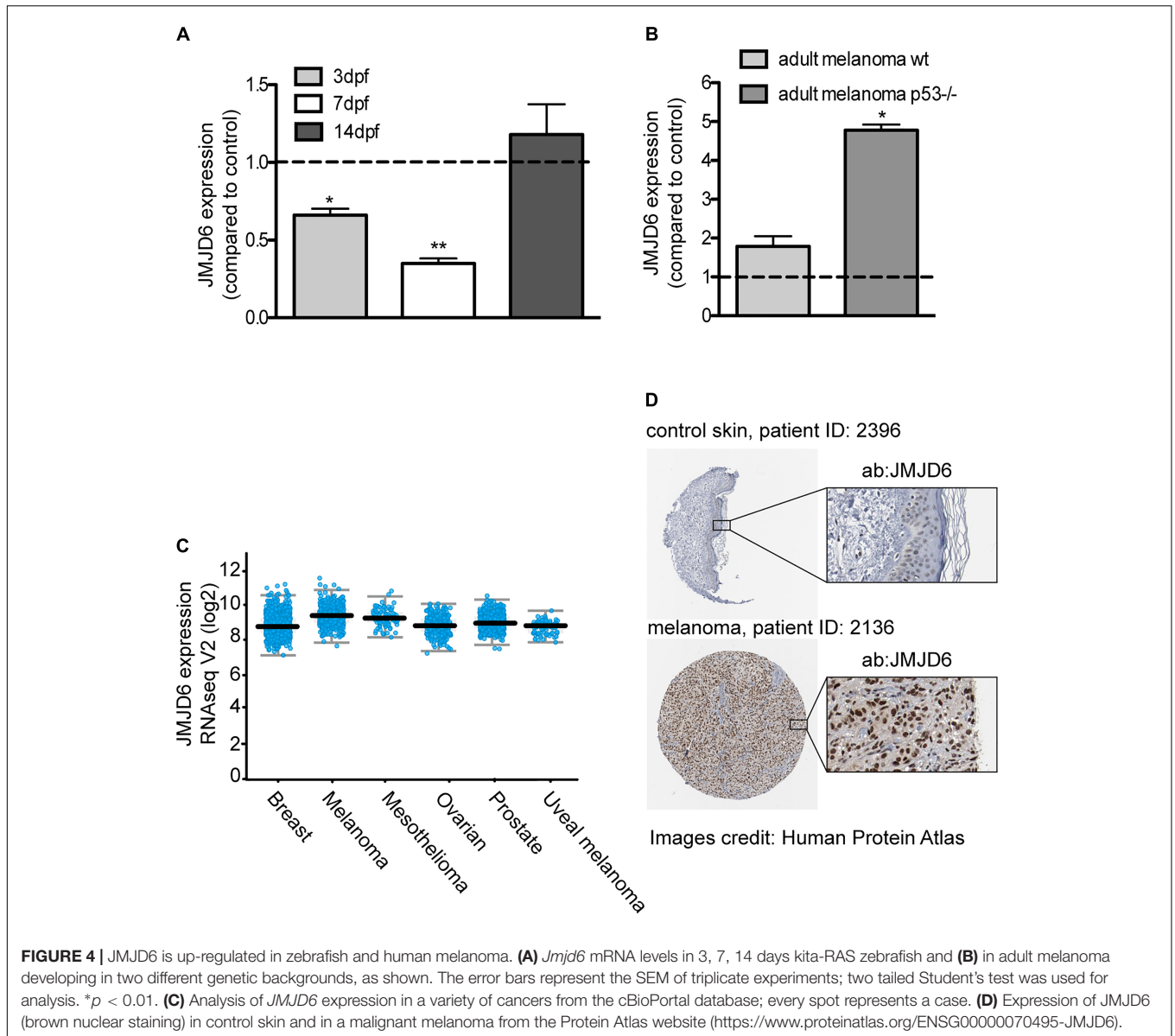


(Supplementary Figure S3A, column 2) and *jmj6* protein levels (Supplementary Figure S3B, lane 2). To test if *jmj6* down-regulation was due to increased expression of miR-146a and/or miR-193a, we reduced microRNA expression by injecting morpholinos (MO) specific to miR-146a or miR-193a and measured *jmj6* mRNA and protein levels in morpholino injected HS-Ras embryos. All morpholinos were able to reduce expression levels of their targets (data not shown) and to increase the levels of *jmj6* transcripts, repressed by ras, to levels similar to controls (Supplementary Figure S3A, columns

3–4) and protein levels (Supplementary Figure S3B, lanes 3–4), suggesting that ras-induced miRs are responsible for the downregulation of *jmj6* levels observed in response to ras expression.

Jmjd6 in Melanoma

In our model of melanoma progression, where ras is overexpressed in melanocytes, *jmj6* levels are reduced compared to control larvae at 3 and 7 dpf (Figure 4A). However, at 14 dpf, there is no significant difference in *jmj6* levels between kita:Ras



and controls. We then analyzed the levels of *jmjd6* expression in full-blown melanoma in two different genotypes: wild type ($p53^{+/+}$) and $p53^{-/-}$. In the latter background, melanomas developed earlier and were highly invasive from the earliest stages (Santoriello et al., 2010). QPCR analysis of *jmjd6* levels in six wild type and in three $p53^{-/-}$ cases showed significantly higher levels of expression of *jmjd6* in melanoma, especially in tumors developing in a $p53^{-/-}$ genetic background (Figure 4B).

Given the unexpected increase of *jmjd6* expression in melanoma, and its correlation with a more aggressive phenotype (Liu et al., 2017), to understand the clinical relevance of our findings, we queried online databases to investigate the expression levels of miR-146a, miR-193a and JMJD6 in melanoma samples from human patients. Data reported here on human melanoma are derived from publicly available resources, as stated in the following text and in the figure's legend. While

no changes in miR-193a expression were reported in melanoma, a couple of studies (GSE18509 and GSE31568, see dbDEMC at www.picb.ac.cn/dbDEMC/index.html) reported an increase of miR-146a in melanoma (not shown). Next, we analyzed the expression levels of JMJD6 in different types of cancers, including melanoma, using the website cBioPortal for Cancer Genomics⁶ (Cerami et al., 2012). As shown in Figure 4C, we found that JMJD6 is upregulated in different cancers, with melanoma being one of the cancer having higher levels of JMJD6 expression and high genomic alteration frequency (with amplification in almost 3% of cases, Supplementary Figure S4A). Looking carefully into the skin cutaneous melanoma TCGA dataset we found that the levels of *JMJD6* are upregulated in 16% of human cutaneous melanoma (72 out of 469 patients, Supplementary Figure S4B).

⁶<http://www.cbioportal.org/>

Moreover, *JMJD6* expression levels are higher in the samples with HRAS and BRAF mutations compared to samples with *wild type* HRAS and BRAF (**Supplementary Figures S4C,D**), suggesting that *JMJD6* is upregulated by RAS signaling in these melanomas. Patients with alteration of *JMJD6* (mutations, amplifications, deep deletions, or multiple alterations) have a worse overall survival and disease/progression-free survival compared with patients with wild type *JMJD6* (**Supplementary Figures S4E,F**), suggesting a key role of *JMJD6* in disease progression.

Next, we investigated the levels of *JMJD6* protein in human melanoma using the website Protein Atlas⁷ (Uhlen et al., 2017). The website reported medium (in three patients) or high (in nine patients) nuclear *JMJD6* immunostaining in malignant melanoma. An example of a high *JMJD6* immunostaining in melanoma is shown in comparison to control skin (where *JMJD6* is not expressed) (**Figure 4D**) (Uhlen et al., 2017). These data suggest that the microRNA-mediated downregulation of *jmjd6* in the zebrafish progressive melanoma model is a transient event and at later stages of melanoma development or in more aggressive melanomas in fish and in human, *Jmjd6* is overexpressed.

Expression of miR-Resistant *Jmjd6* Promotes Ras-Induced Melanoma

Given the dynamic changes in *Jmjd6* expression in the Ras-induced melanoma model in zebrafish, and the overall increase in expression in human melanoma, we wanted to clarify the role of *Jmjd6* in melanoma with a gain of function approach. Therefore, we produced a transgenic line that expresses miR (146a and 193a) -resistant *jmjd6* in melanocytes. This was achieved by replacing the 3' UTR of *jmjd6* in the transgenic construct with an artificial sequence (SV40 polyA, **Figure 5A**). With this construct, we generated a *tg(UAS:eGFP-jmjd6)* transgenic line using standard Tol2 transposase methods (Kawakami, 2004), and crossed it to *kita:Gal4* fish. The double transgenic fish, designated as *kita:Jmjd6*, have no phenotype; however *eGFP-Jmjd6* expression was confirmed by *kita* driven GFP nuclear localization in melanocytes and notochord cells (**Figures 5B–D**). To study the effects of combined expression of oncogenic ras and *Jmjd6* in melanoma we generated triple transgenic fish, *Et(kita:Gal4TA, UAS:mCherry)^{hmz1};Tg(UAS:eGFP-HRASV12)^{io006}; Tg(UAS:eGFP-JMJD6)^{ka202}* (designated as *kita/Ras/Jmjd6*, **Figure 5E**) and observe the fish for the development of melanoma at regular intervals, from 7 days to 1 month. As shown in the disease-free survival curve, 60% of double transgenic *kita-ras* fish show melanoma at 1 month (**Figure 5F**). However, triple transgenic fish *kita/Ras/Jmjd6* developed melanoma at an earlier stage (**Figures 5E,F**) and by 1 month of age, penetrance of melanoma was 95% (**Figure 5F**). The tumors appeared in multiple locations in the same fish (**Figure 5E**) and were more invasive, as judged by the body surface showing melanoma lesions and by histological analysis (**Figures 5G,H**).

We also noticed that *Kita/Ras/Jmjd6* melanomas have massive infiltration of leukocytes (L-plastin+ cells), resembling

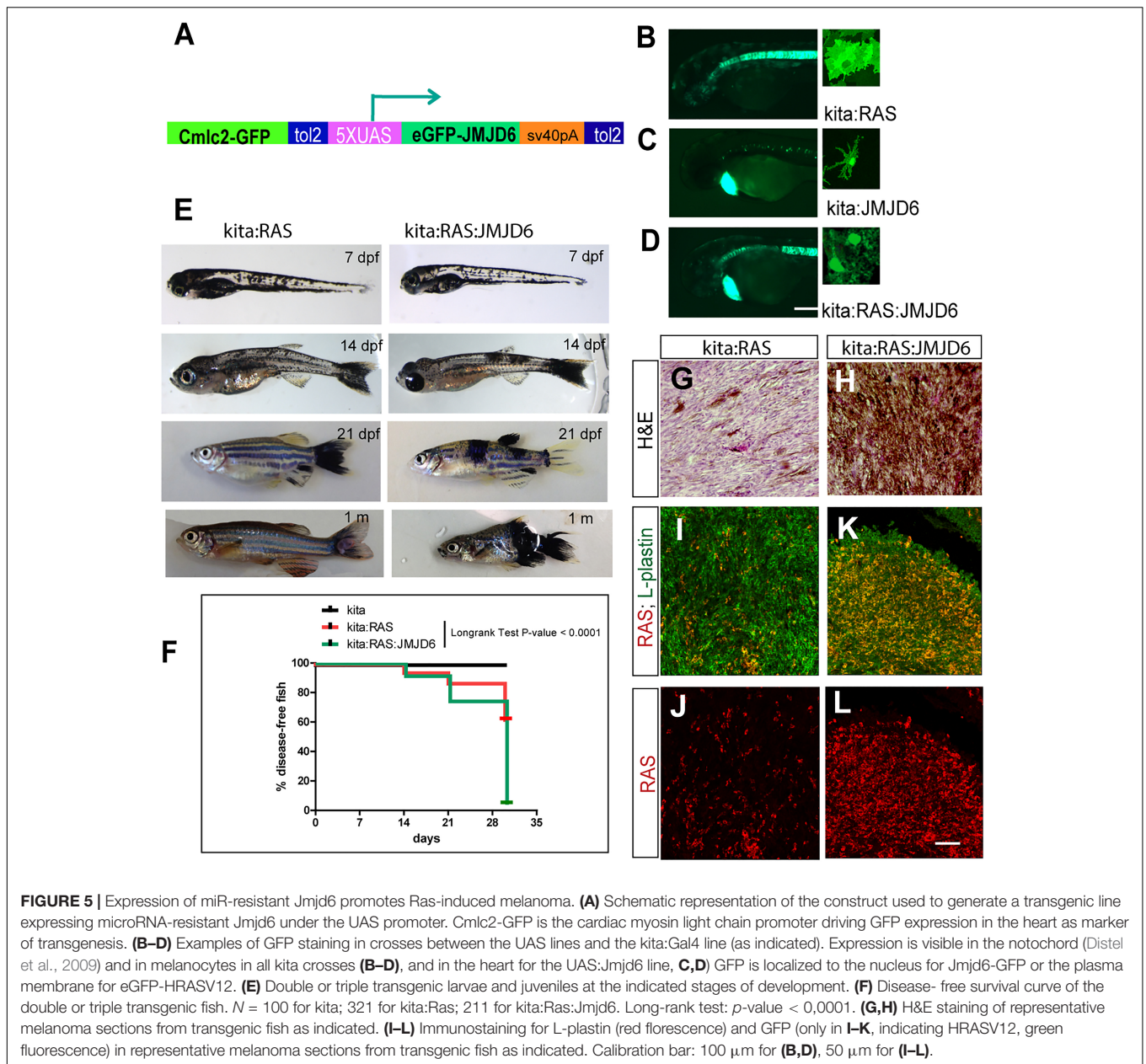
macrophages and neutrophils for their shape, much higher than in to *Kita/Ras* melanomas (**Figures 5I–L**).

DISCUSSION

In this study we used a progressive model of melanoma in zebrafish to study the changes of microRNA expression at the onset of RAS-induced transformation and throughout progression of the disease. We found six microRNAs, which are upregulated as an early response to oncogenic RAS expression in three different models. As two of these microRNAs target *Jmjd6* we investigated the significance of these interactions for melanoma progression. To our surprise we discovered that the target of these increased microRNAs, *Jmjd6*, is overexpressed in aggressive zebrafish melanoma. This suggested that overexpression of *Jmjd6* promotes melanoma progression and that the increase of the microRNAs that downregulate *Jmjd6* at the onset of Ras expression is part of a defensive response against the pro-oncogenic activity of *Jmjd6*. We validated this hypothesis by generating triple transgenic zebrafish that express micro-RNA resistant *Jmjd6*. Melanoma develop faster in the *kita/ras/jmjd6* fish, supporting a pro-oncogenic role of *Jmjd6*. Further work is needed to clarify how *Jmjd6* favors melanoma development.

Jmjd6 is a JumanjiC-domain containing protein, which has been endorsed for different functions. It was initially identified as a phosphatidyserine receptor (PSR) on the surface of phagocytes (Fadok et al., 2000). Ablation of *Jmjd6* in mice, and morpholino downregulation of *Jmjd6/PSR* in zebrafish (Hong et al., 2004) causes abnormal development and leads to neonatal lethality in mouse (Böse et al., 2004; Kunisaki et al., 2004). However, many lines of evidence argue against a function of *Jmjd6* as a PSR, primarily its nuclear localization (Cui et al., 2004; Tibrewal et al., 2007), and a number of newly reported nuclear activities. Subsequently, *Jmjd6* was shown to function as an arginine demethylase, which removes repressive symmetric methylation marks from histone 2 (H2R3me2s) and histone 4 (H4R3me2s) arginines (Chang et al., 2007), but other groups have been unable to confirm the arginine demethylation activity of *JMJD6* (Hahn et al., 2010). Webby et al. (2009) reported that *JMJD6* acts as a lysyl-5-hydroxylase of the splice factor subunit U2A65. Silencing of *JMJD6* expression in endothelial cells resulted in abnormal splicing of the VEGF receptor 1 (Boeckel et al., 2011). Meanwhile, a structural study suggested that methyl groups on single-stranded RNAs (ssRNAs) might be substrates of *JMJD6* (Hong et al., 2010). More recently, a proteomic approach identified *JMJD6* as one of a few binding partners of the bromodomain and extraterminal (BET) domain protein Brd4 (Rahman et al., 2011), which regulates gene expression through interaction with the cdk9 subunit of the positive transcription and elongation factor, pTEFb complex (Jang et al., 2005). Further studies lead to the identification of *JMJD6* as the partner of BRD4 in binding distal enhancers known as anti-pause enhancers, which regulate release from transcriptional pausing in a large subset of transcriptional units which depend on long-range interactions (Liu et al., 2013). Here, the demethylase activity of *JMJD6* on

⁷<https://www.proteinatlas.org/>



the snRNA, 7SK, results in the disassembly of the transcriptional repressive complex HEXIM1-7SK, releasing pTEFb from pausing (Liu et al., 2013). It would be interesting to study whether anti-pause enhancers, which are the substrates of the JMJD6-Brd4 interaction, are associated with pro-oncogenic gene expression in melanoma. Given the robust correlation between *Jmjd6* overexpression and aggressive melanoma in different models and in human samples, it would be important to clarify if the pro-oncogenic function of JMJD6 depends on this transcriptional activity. More recently, Liu et al. (2017) have shown that the JMJD6 promotes melanomagenesis through the regulation of the alternative splicing of PAK1, a key MAPK signaling component. In recent years, also RNA binding abilities of *Jmjd6* are emerging, perhaps its many functions, linked to arginine methylation of

RNA binding proteins in transcription initiation complexes, spliceosome and ribosomes may be mediated by its RNA-binding abilities. Indeed Heim et al. (2014), showed that treatment with RNase disrupt *Jmjd6* nuclear localization.

In our study we found that two microRNAs induced by Ras (miR-146a and miR-193a) behave as tumor suppressors. MiR-146a and b are well-studied for their roles in immune responses. Induced by inflammation and infection through NF-κB signaling (Bhaumik et al., 2008), miR-146a, and to a lesser extent miR-146b, function in a negative feedback loop to downregulate several pro-inflammatory effectors. Indeed miR-146a has been implicated in attenuating pro-inflammatory responses (Saba et al., 2014), which could contribute in cancer to the elimination of early transformed cells by the immune system, and in reducing the

metastatic potential of breast cancer cells (Bhaumik et al., 2008). Increase in expression of miR-146a was reported in unclassified melanoma samples (Philippidou et al., 2010), and found to suppress brain metastasis from melanoma in experimental models (Hwang et al., 2013). These findings support a tumor suppressor role for miR-146a in melanoma. Our study provides evidence that miR-146a is induced by the same MAPK/AKT pathway that sustains melanoma growth at the earliest stages of transformation, when it could exert an anti-melanoma function by repressing *Jmjd6* and perhaps also pro-tumoral inflammation. The tumor suppressive activity of miR-193a has been related to its ability to inhibit cell proliferation and to promote apoptosis of cancer cells (Nakano et al., 2013; Mamoori et al., 2018). MiR-193a undergoes epigenetic silencing in acute myeloid leukemia by the AML1/ETO fusion protein (Li et al., 2013), where miR-193 was found to repress several pro-leukemogenic factors, including KIT. Moreover miR193a has been found to participate in a regulatory loop that controls p53 family member levels (Ory et al., 2011) thus further reinforcing the hypothesis that miR193a is a tumor suppressor. The finding that both microRNAs target *Jmjd6* and that this regulation is conserved in zebrafish and human melanoma suggests that lowering JMJD6 levels in cancer is another function of the tumor suppressors miR-146a and miR-193a.

The mechanisms through which *Jmjd6* promote melanoma progression is still unknown. Different approaches, including transcriptome, epigenome and spliceosome analysis, can help to gain insights into the pro-oncogenic activity of JMJD6. In these studies, the transgenic lines *kita:Jmjd6* and *kita/Ras/Jmjd6* will provide a source of GFP tagged *Jmjd6* proteins expressed specifically in melanocytes. We were puzzled by the massive presence of L-plastin positive cells (leukocytes, possibly including neutrophils and macrophages) within the *kita/Ras/Jmjd6* melanomas, compared to *kita/Ras* melanomas. Neutrophils and eosinophil infiltrations in melanoma predict unfavorable disease outcome (Ding et al., 2018) whereas accumulation of dendritic cells and T-lymphocytes is positively correlated with survival. Therefore, the increase of L-plastin positive neutrophils and macrophages is an index of the aggressiveness of these tumors. It is intriguing that one of the microRNAs targeting *Jmjd6* in this progressive model of melanoma is miR-146a, a well-known regulator of inflammatory responses. It would be interesting to investigate whether miR-146a levels differ in melanoma developing in *kita/Ras* (where they are increased according to RNA-Seq data) versus those developing in *kita/Ras/Jmjd6*.

In summary, this study has shown that several microRNAs are induced by RAS signaling in melanoma initiating cells at the onset of transformation. Induced miR-146a and -193a target *Jmjd6*, which is temporarily downregulated. At later stages of melanoma development, and in human malignant melanoma with unfavorable prognosis, *Jmjd6* is overexpressed, and in a zebrafish model where melanocytes express both Ras and *Jmjd6*, melanomas are more aggressive. Therefore, *Jmjd6* has pro-oncogenic activities and the initial downregulation mediated by microRNAs may be part of an anti-oncogenic response, which is induced by the same RAS oncogene.

MATERIALS AND METHODS

Zebrafish Lines

Zebrafish were maintained and staged as described (Kimmel et al., 1995).

In addition to wild type AB fish, we used the following lines:

- *Et(kita:Gal4TA, UAS:mCherry)^{hmz1}; Tg(UAS:eGFP-HRASV12)^{io006}* a double transgenic line in which oncogenic ras expression is regulated by the *kita* promoter and that develop melanoma (Santoriello et al., 2010), also crossed to *ZDF1 (p53^{m214k/+})* (Berghmans et al., 2005).
- *Tg(hsp70l:EGFP-HRAS_G12V)^{io3}* an heat-inducible oncogene expressing line (Santoriello et al., 2009).
- *Et(zic4:Gal4TA4, UAS:mCherry)^{hzm5}; Tg(UAS:eGFP-HRASV12)^{io006}* a double transgenic line in which oncogenic ras expression is regulated by the *zic4* promoter and that develop glioma (Mayrhofer et al., 2017).
- *Et(kita:Gal4TA, UAS:mCherry)^{hmz1}; Tg(UAS:eGFP-Jmjd6)^{ka202}*; and *Et(kita:Gal4TA, UAS:mCherry)^{hmz1}; Tg(UAS:eGFP-HRASV12)^{io006}; Tg(UAS:eGFP-Jmjd6)^{ka202}* double and triple transgenic lines in which the expression of a microRNA resistant *Jmjd6* is regulated by Gal4 expressed under the *kita* promoter alone (double) or together with HRASV12 (triple), generated in the course of this study. This study was carried out in accordance with the recommendations of the OPBA of the University of Trento on Animal Welfare. Experimental procedures on zebrafish were performed in accordance with the European law on Animal Protection and Authorization No. 75/2017-PR from the Italian Ministry of Health.

miRNA Array

Custom-designed 8 × 15k microarray slides were ordered from Agilent Technologies. The 15k custom design was obtained from Edwin Cuppen and Eugene Berezikov (Hubrecht Institute, Utrecht, Netherlands) and has been submitted into the Gene Expression Omnibus (GEO) database (GPL 15403). The 15k design contained a duplicate of 7604 probes of 60-oligonucleotide length. The probes consisted of 2 × 22 nucleotide sequences antisense to mature miRNAs separated by a spacer of 8 nucleotides (CGATCTTT) and with a second spacer with the same sequence at the end. From 7604 probes 546 were designed for left (5') and right (3') arms of the hairpins of zebrafish miRNAs that are known in miRBase, while the remainder 7058 probes corresponded to predicted hairpin structures in the zebrafish genome that might include additional miRNAs but were not considered in this study. Total RNA, including microRNA, were extracted from 3-7-14 dpf wt or UAS-RAS larvae (driven by *kita:Gal4*, *zic:Gal4*, or *hsp:Gal4*), and from adult melanoma or wt fin tissue using miRNeasy Mini Kit® (Qiagen). Three biological replicates were obtained for each condition. For dual color hybridization of the Agilent chips miRNA samples from RAS transgenics were labeled with Hy3 and samples from control fish were labeled with Hy5 with miRCURY™ LNA microRNA, Hy3™/Hy5™ Power Labeling kit (Exiqon) using 1 microgram of total RNA according to the manufacturer's instructions.

The dual color hybridization of the microarray chips was performed according to Agilent protocol GE2_105_Jan09⁸ for two-color microarray-based gene expression analysis except that hybridization and washing was performed at 37°C. The arrays were scanned with DNA Microarray Scanner G2565CA from Agilent Technologies. The arrays were scanned twice with 10% PMT and 100% PMT laser power. Microarray data was processed from raw data image files with Feature Extraction Software 9.5.3.1 (Agilent Technologies). The XDR function was used to extend the dynamic range. Processed data were subsequently imported into Rosetta Resolver 7.1 (Rosetta Biosoftware, Seattle, WA, United States) and subjected to default ratio error modeling. The raw data have been submitted to GEO under accession number GSE 37015. Values above 1.2 log₂ Fold Changes and *p*-values < 0.01 in all three models were used as selection criteria.

QPCR for MicroRNAs

To confirm microarray data, total RNA, including miRNA, were purified from 3 dpf embryos using miRNeasy Mini Kit[®] (Qiagen). Mature miRNA were reverse transcribed using specific primers mix for each miR to produce different cDNA for TaqMan[®] MicroRNA assay (30 ng of total mRNA for each reaction) (Applied Biosystems). Taqman probes were designed for the active strand (−5p) of miR-21, miR-146a, and miR-146b and for the active (−3p) strand of miR-193a. Real-time PCR reactions based on TaqMan reagent chemistry were performed in duplicate on ABI PRISM[®]7900HT Fast Real-Time PCR System (Applied Biosystems). The level of miRNA expression was measured using *C_T* (cycle threshold). For normalization, miR-133, which was unaffected by RAS overexpression, was taken as reference. Fold change was generated using the equation 2^{−*C_T*}. The list of oligos used and their sequences is provided in **Supplementary Table S2**.

Inhibitor Treatment

Three dpf HS-RAS and AB embryos were incubated in 2ml E3 medium in a 12 well plate in the presence of the following inhibitors: 1 μg/ml PD98059 (Calbiochem), 15 μM LY294002 (Cell Signaling) and 1 μM Rapamycin (Tocris). After 2 h, embryos were heat-shocked at 39°C for 30 min. After 6 h 50 RAS-GFP+ or GFP- embryos were collected in Trizol or sample buffer (2% SDS, 10% glycerol, 60 mM Tris pH 6.8) for miRNA or protein extraction respectively.

Western Blot and Antisera

Ten 3 dpf embryos were homogenized in 200 μl sample buffer (2% SDS, 10% glycerol, 60 mM Tris pH 6.8). 30 μg of total extract were resolved by SDS-PAGE, transferred to nitrocellulose and tested with the following antibodies: phospho-p44/42 (1:1000, Cell Signaling), p44/42 (1:1000, Cell Signaling), Phospho-AKT (1:1000, Cell Signaling), AKT (1:1000, Cell Signaling), Phospho-S6 (1:1000, Cell Signaling), S6 (Cell Signaling 1:1000), *jmjd6* (Abcam, 1:1000), GFP (1:1000, Torrey Pines, United States), actin (1:5000, MP Biomedical).

⁸www.Agilent.com

Manual Inspection of 3' UTR of Candidate MicroRNA Targets

An initial analysis performed with MicroCosm (now incorporated in tools4mirs at <https://tools4mirs.org/>) which used a previous version of the zebrafish genome identified a few genes as potential targets of both miR146a and 193a. Manual inspection of the 3' UTR regions of these genes using the GRCz11 release at Ensembl⁵ confirmed that only *jmjd6* 3' UTR region contained sequences that match the seed regions of both microRNAs. We then used a web-based interaction-prediction algorithm for RNA molecules, IntaRNA⁴ (Mann et al., 2017) for the fast and accurate prediction of the interactions between miR-146a and/or 193a with *jmjd6* mRNAs (*Ensemble, ENSDARG00000102896*⁵). We followed the web-site instructions and used *jmjd6* and miR-146a-5p and -193a-3p sequences as input. The following parameters were used: minimum number of base pairs in seed: 7; temperature for energy computation: 37°C; energy parameter set (Vienna package), Turner Model 2004 (Lorenz et al., 2011); energy interaction levels < −8.

Morpholino, Duplexes, and Plasmids

Morpholinos, including a standard control morpholino, were obtained from Gene Tools (United States), titrated to non-toxic concentrations and injected in a final volume of 2 nl per 1-cell embryo. A list of all morpholinos, their sequences and the concentration used is provided in **Supplementary Table S3**. Synthetic miR- duplexes controls and 146a were designed and ordered from SIGMA (United States). Synthetic miR- duplexes for miR-193a were purchased from Ambion. Duplexes were dissolved in RNase free water and diluted using annealing buffer (30 mM HEPES-KOH pH 7.4, 10 mM KCl, 2 mM MgCl₂, 50 mM NH₄Ac) to a final concentration of 10 μM for miR-146a 5 μM for miR-193a. The solution was incubated for 1 min at 90°C, cooled down slowly to room temperature and injected in a final volume of 2 nl per 1-cell embryo. A list of all duplexes, their sequences and the concentration used is provided in **Supplementary Table S4**.

For *Jmjd6* reporter construct, the whole *Jmjd6* (*Ensemble, ENSDARG00000102896*) 3' UTRs was PCR amplified from cDNA using specific primers (**Supplementary Table S2**). The PCR product was subcloned into the pCS2:eGFP vector downstream of the GFP open reading frame and confirmed by sequencing.

Generation of a *Jmjd6* Transgenic Line

To express a microRNA resistant *Jmjd6* in melanocytes, the full coding region excluding the stop codon of *Jmjd6* (*Ensemble, ENSDARG00000102896*) was PCR amplified and cloned into *pEntry5-no stop* (Invitrogen) and then recombined using gateway technology with a *pEnt5-4nrUAS* (generated by cloning four non-repetitive UAS elements into pENT5' from Invitrogen), a *p3E-EGFPpA* (Tol2Kit clone n.366) + *pDestTol2CG2* (Tol2Kit clone n. 395) using gateway (Kwan and North, 2017). Clone numbers and sequences can be found at: http://chien.neuro.utah.edu/tol2kitwiki/index.php/Main_Page.

Final recombined clones were checked by sequencing. *4nrUAS:eGFP-Jmjd6* plasmid was injected in 1-cell embryos

of the *Et(kita:Gal4TA, UAS:mCherry)^{hmz1}* line to generate a transgenic line using standard Tol2 mediated transgenesis (Kawakami, 2004; Pase and Lieschke, 2009).

Zebrafish Embryo Injections

Zebrafish embryos at the stage of 1–2 cells were injected with morpholinos against miRs or *Jmjd6* diluted in double distilled, sterile H₂O. The morpholino oligonucleotides were injected at a concentration of 5 ng/nl, in a volume of 2 nl/embryo. miR duplexes mimicking mature microRNA were injected following a described protocol (Pase and Lieschke, 2009), at a concentration of 10 μM for miR-146a and miR-146b and 5 μM for miR193a in a volume of 2 nl/embryo.

Sensor injections: mRNA encoding for eGFP carrying *Jmjd6* 3' UTR was *in vitro* synthesized and injected in 1–2 cell zebrafish embryos at 100 pg/embryo, alone or in combination with duplexes or morpholinos.

Imaging

Photographs of whole larvae were acquired with a Nikon S100 stereomicroscope equipped with epifluorescence and multiple filters. We used a Leica SP5 confocal for analysis of melanocytes expressing Ras-eGFP, *Jmjd6*-GFP, and L-plastin immunoreactivity.

AGO2 – RIP

One hundred 3 dpf embryos injected or not with miR duplex were homogenized in ice-cold buffer A containing 50 mM Tris-HCl pH 7.5, 5 mM EDTA, 5 mM EGTA, complete proteinase inhibitor (Roche) and 1 U/μl RNase inhibitor SUPERnase-IN (Ambion). Unbroken cells were removed at 100 g for 5 min at 4°C. NP40 was added at 0.5% (wt/vol) and samples incubated at 4°C for 15 min with rotation and centrifuged at 10000 × g for 15 min. SN was transferred to a new tube and the protein were measured by BCA. 2 mg of protein were diluted with buffer A and incubated overnight at 4°C with 50 μl Dynabeads (Invitrogen) bound with 2 μg Ago2 antibody (Abcam) or IgG (negative control). The next morning beads were washed four times with 1 ml of washing buffer containing 50 mM Tris-HCl pH 7.4, 150 mM NaCl, 1 mM MgCl₂ and 0.05% NP40. Beads were then resuspended in 1ml of washing buffer and 200 μl of beads were pelleted and resuspended in 50 ul sample buffer to test Ago2 by western blot (Abcam 1:1000). The remaining 800 ul were resuspend with 500 μl of trizol and RNA was extracted by RNeasy micro Kit (Qiagen). All the RNA was retro-transcribed using Vilo (Invitrogen) and 1 μl of cDNA was used for PCR using specific primers for *jmd6* or the housekeeping gene, *gapdh*.

Analysis of Data From cBioportal and Protein Atlas

Analysis of JMJD6 expression, correlation with HRAS or BRAF mutations, survival and disease/progression-free survival in patients was done using the dataset Skin Cutaneous Melanoma TCGA dataset in cBioportal⁶. The survival and disease/progression-free survival were done taking into account

the following JMJD6 alterations: mutations, amplifications, deep deletions or multiple alterations.

We report here examples of JMJD6 protein localization in control skin (ID: 2396⁹) and in a malignant melanoma (ID: 2136¹⁰) from the Protein Atlas website.

AUTHOR CONTRIBUTIONS

VA and MM design the study, conducted experiments, and wrote the manuscript. VA, AO and AM performed the microarray analysis. SK, LS, and VG performed bioinformatics analysis. MS and AM provided conceptual insights.

FUNDING

Work in the lab of MCM is supported the European Commission under the Horizon 2020 program (U. M. Cure/Project No. 667787), and by a 5 × 1000 LILT-2016 contribution. AM acknowledges the contribution of the European Commission 6th Framework Project ZF-TOOLS (LSHG-CT-2006-037220).

ACKNOWLEDGMENTS

We would like to thank Cristina Santoriello for help and discussion on the experimental design, Nadine Borel and EZRC personnel for fish care, Reinhard Koester and Martin Distel for sharing the Gal4 lines used in this study, Kyuson Yun for reading and commenting on an earlier version of the manuscript, Erik Dassi for help with the heatmap in **Figure 1**, and Sabrina Burkart for technical support.

SUPPLEMENTARY MATERIAL

The Supplementary Material for this article can be found online at: <https://www.frontiersin.org/articles/10.3389/fgene.2018.00675/full#supplementary-material>

FIGURE S1 | Output of IntaRNA website, showing interaction of microRNAs 146a (**A**) and 193a (**B**) with the 3' UTR of *jmd6*. An energy of –8 Kcal/mol or less is indicative of a stable interaction.

FIGURE S2 | Injections of duplexes microRNAs cause increase of the corresponding microRNAs and mild developmental defects. (**A**) QPCR analysis of the expression levels of the microRNAs indicated. (**B**) All the other injected embryos developed without visible abnormalities.

FIGURE S3 | *Jmjd6* is down-regulated upon Ras expression. *Jmjd6* mRNA (**A**) and protein levels (**B**) are downregulated by Ras overexpression (2nd lane) and rescued to normal levels by downregulating the increased microRNAs (lanes 3–4).

⁹<https://www.proteinatlas.org/ENSG00000070495-JMJD6/tissue/skin>

¹⁰<https://www.proteinatlas.org/ENSG00000070495-JMJD6/pathology/tissue/melanoma#img>

FIGURE S4 | cBioPortal data of JMJD6. **(A)** Alteration frequency of JMJD6 in different type of cancers. **(B)** JMJD6 expression in melanoma patients; each bar represents a patient. Red bars: patients with upregulated JMJD6. Blue bars: patients with downregulated JMJD6. JMJD6 expression in HRAS **(C)** and BRAF **(D)** mutated melanoma. Overall survival **(E)** and disease/progression-free survival **(F)** in patients with (red curve) or without (blue curve) JMJD6 alterations.

TABLE S1 | miRNA array results table. Column A: probe ID; column B: sequence of the probe; column C: Gene ID; column D: Gene symbol; Columns E–P: fold change and relative *p*-value of the samples as indicated. Fold change and *p*-value are calculated by comparing the miRNAs expression in *kita*-Ras larvae at 3, 7, and 14 dpf, HS-Ras, and *zic* at 3 dpf and adult melanoma with the respective control

(AB for all the larvae and skin from adult AB wild type fish for the adult melanoma). MicroRNAs selected for further studies (see text for criteria used) and their expression values (log2FoldChanges and *p*Values) are highlighted.

TABLE S2 | Oligo sequences. Sequences of the oligos used for qPCR, RIP assay, *jmjd6* 3'-UTR cloning and Gateway cloning of *Jmjd6*.

TABLE S3 | Morpholino sequences. Sequences of the morpholinos used in the study.

TABLE S4 | microRNA duplexes. Sequences of the miR control (miR-C) and miR-146a₁ injected in the embryos. The sequence of miR-193a was not provided by the supplier (Ambion).

REFERENCES

- Berghmans, S., Murphey, R. D., Wienholds, E., Neuberg, D., Kutok, J. L., Fletcher, C. D. M., et al. (2005). tp53 mutant zebrafish develop malignant peripheral nerve sheath tumors. *Proc. Natl. Acad. Sci. U.S.A.* 102, 407–412. doi: 10.1073/pnas.0406252102
- Bhaumik, D., Scott, G. K., Schokrpur, S., Patil, C. K., Campisi, J., and Benz, C. C. (2008). Expression of microRNA-146 suppresses NF-kappaB activity with reduction of metastatic potential in breast cancer cells. *Oncogene* 27, 5643–5647. doi: 10.1038/onc.2008.171
- Boeckel, J.-N., Guarani, V., Koyanagi, M., Roexe, T., Lengeling, A., Schermuly, R. T., et al. (2011). Jumonji domain-containing protein 6 (*Jmjd6*) is required for angiogenic sprouting and regulates splicing of VEGF-receptor 1. *Proc. Natl. Acad. Sci. U.S.A.* 108, 3276–3281. doi: 10.1073/pnas.1008098108
- Böse, J., Gruber, A. D., Helming, L., Schiebe, S., Wegener, I., Hafner, M., et al. (2004). The phosphatidylserine receptor has essential functions during embryogenesis but not in apoptotic cell removal. *J. Biol.* 3:15. doi: 10.1186/jbiol10
- Cerami, E., Gao, J., Dogrusoz, U., Gross, B. E., Sumer, S. O., Aksoy, B. A., et al. (2012). The cBio cancer genomics portal: an open platform for exploring multidimensional cancer genomics data. *Cancer Discov.* 2, 401–404. doi: 10.1158/2159-8290.CD-12-0095
- Chang, B., Chen, Y., Zhao, Y., and Bruck, R. K. (2007). JMJD6 is a histone arginine demethylase. *Science* 318, 444–447. doi: 10.1126/science.1145801
- Chin, L., Artandi, S. E., Shen, Q., Tam, A., Lee, S. L., Gottlieb, G. J., et al. (1999a). deficiency rescues the adverse effects of telomere loss and cooperates with telomere dysfunction to accelerate carcinogenesis. *Cell* 97, 527–538.
- Chin, L., Tam, A., Pomerantz, J., Wong, M., Holash, J., Bardeesy, N., et al. (1999b). Essential role for oncogenic Ras in tumour maintenance. *Nature* 400, 468–472. doi: 10.1038/22788
- Cui, P., Qin, B., Liu, N., Pan, G., and Pei, D. (2004). Nuclear localization of the phosphatidylserine receptor protein via multiple nuclear localization signals. *Exp. Cell Res.* 293, 154–163. doi: 10.1016/j.yexcr.2003.09.023
- Ding, Y., Zhang, S., and Qiao, J. (2018). Prognostic value of neutrophil-to-lymphocyte ratio in melanoma: evidence from a PRISMA-compliant meta-analysis. *Medicine* 97:e11446. doi: 10.1097/MD.00000000000011446
- Distel, M., Wullmann, M. F., and Köster, R. W. (2009). Optimized Gal4 genetics for permanent gene expression mapping in zebrafish. *Proc. Natl. Acad. Sci. U.S.A.* 106, 13365–13370. doi: 10.1073/pnas.0903060106
- Fadok, V. A., Bratton, D. L., Rose, D. M., Pearson, A., Ezekewitz, R. A., and Henson, P. M. (2000). A receptor for phosphatidylserine-specific clearance of apoptotic cells. *Nature* 405, 85–90. doi: 10.1038/35011084
- Frezzetti, D., De Menna, M., Zoppoli, P., Guerra, C., Ferraro, A., Bello, A. M., et al. (2011). Upregulation of miR-21 by Ras *in vivo* and its role in tumor growth. *Oncogene* 30, 275–286. doi: 10.1038/onc.2010.416
- Hahn, P., Wegener, I., Burrells, A., Böse, J., Wolf, A., Erck, C., et al. (2010). Analysis of *Jmjd6* cellular localization and testing for its involvement in histone demethylation. *PLoS One* 5:e13769. doi: 10.1371/journal.pone.0013769
- Harrandah, A. M., Mora, R. A., and Chan, E. K. L. (2018). Emerging microRNAs in cancer diagnosis, progression, and immune surveillance. *Cancer Lett.* 438, 126–132. doi: 10.1016/j.canlet.2018.09.019
- Heim, A., Grimm, C., Müller, U., Häußler, S., Macken, M. M., Merl, J., et al. (2014). Jumonji domain containing protein 6 (*Jmjd6*) modulates splicing and specifically interacts with arginine-serine-rich (RS) domains of SR- and SR-like proteins. *Nucleic Acids Res.* 42, 7833–7850. doi: 10.1093/nar/gku488
- Hong, J.-R., Lin, G.-H., Lin, C. J.-F., Wang, W.-P., Lee, C.-C., Lin, T.-L., et al. (2004). Phosphatidylserine receptor is required for the engulfment of dead apoptotic cells and for normal embryonic development in zebrafish. *Development* 131, 5417–5427. doi: 10.1242/dev.01409
- Hong, X., Zang, J., White, J., Wang, C., Pan, C.-H., Zhao, R., et al. (2010). Interaction of JMJD6 with single-stranded RNA. *Proc. Natl. Acad. Sci. U.S.A.* 107, 14568–14572. doi: 10.1073/pnas.1008832107
- Hwang, S. H., Lee, B.-H., Kim, H.-J., Cho, H.-J., Shin, H.-C., Im, K.-S., et al. (2013). Suppression of metastasis of intravenously-inoculated B16/F10 melanoma cells by the novel ginseng-derived ingredient, gintonin: involvement of autotaxin inhibition. *Int. J. Oncol.* 42, 317–326. doi: 10.3892/ijo.2012.1709
- Ikeda, K., Satoh, M., Pauley, K. M., Fritzler, M. J., Reeves, W. H., and Chan, E. K. L. (2006). Detection of the argonaute protein Ago2 and microRNAs in the RNA induced silencing complex (RISC) using a monoclonal antibody. *J. Immunol. Methods* 317, 38–44. doi: 10.1016/j.jim.2006.09.010
- Jang, M. K., Mochizuki, K., Zhou, M., Jeong, H.-S., Brady, J. N., and Ozato, K. (2005). The bromodomain protein Brd4 is a positive regulatory component of P-TEFb and stimulates RNA polymerase II-dependent transcription. *Mol. Cell* 19, 523–534. doi: 10.1016/j.molcel.2005.06.027
- Johnson, L., Mercer, K., Greenbaum, D., Bronson, R. T., Crowley, D., Tuveson, D. A., et al. (2001). Somatic activation of the K-ras oncogene causes early onset lung cancer in mice. *Nature* 410, 1111–1116. doi: 10.1038/35074129
- Kawakami, K. (2004). Transgenesis and gene trap methods in zebrafish by using the Tol2 transposable element. *Methods Cell Biol.* 77, 201–222. doi: 10.1016/S0091-679X(04)77011-9
- Kimmel, C. B., Ballard, W. W., Kimmel, S. R., Ullmann, B., and Schilling, T. F. (1995). Stages of embryonic development of the zebrafish. *Dev. Dyn.* 203, 253–310. doi: 10.1002/aja.1002030302
- Kunisaki, Y., Masuko, S., Noda, M., Inayoshi, A., Sanui, T., Harada, M., et al. (2004). Defective fetal liver erythropoiesis and T lymphopoiesis in mice lacking the phosphatidylserine receptor. *Blood* 103, 3362–3364. doi: 10.1182/blood-2003-09-3245
- Kwan, W., and North, T. E. (2017). Netting novel regulators of hematopoiesis and hematologic malignancies in zebrafish. *Curr. Top. Dev. Biol.* 124, 125–160. doi: 10.1016/bs.ctdb.2016.11.005
- Li, Y., Gao, L., Luo, X., Wang, L., Gao, X., Wang, W., et al. (2013). Epigenetic silencing of microRNA-193a contributes to leukemogenesis in t(8;21) acute myeloid leukemia by activating the PTEN/PI3K signal pathway. *Blood* 121, 499–509. doi: 10.1182/blood-2012-07-444729
- Liu, W., Ma, Q., Wong, K., Li, W., Ohgi, K., Zhang, J., et al. (2013). Brd4 and JMJD6-associated anti-pause enhancers in regulation of transcriptional pause release. *Cell* 155, 1581–1595. doi: 10.1016/j.cell.2013.10.056
- Liu, X., Si, W., Liu, X., He, L., Ren, J., Yang, Z., et al. (2017). JMJD6 promotes melanoma carcinogenesis through regulation of the alternative splicing of PAK1, a key MAPK signaling component. *Mol. Cancer* 16:175. doi: 10.1186/s12943-017-0744-2
- Lorenz, R., Bernhart, S. H., Höner Zu Siederdisen, C., Tafer, H., Flamm, C., Stadler, P. F., et al. (2011). ViennaRNA Package 2.0. *Algorithms Mol. Biol.* 6:26. doi: 10.1186/1748-7188-6-26
- Lukasik, A., Wójcikowski, M., and Zielenkiewicz, P. (2016). Tools4miRs – one place to gather all the tools for miRNA analysis. *Bioinformatics* 32, 2722–2724. doi: 10.1093/bioinformatics/btw189

- Malumbres, M., and Barbacid, M. (2003). RAS oncogenes: the first 30 years. *Nat. Rev. Cancer* 3, 459–465. doi: 10.1038/nrc1097
- Mamoori, A., Gopalan, V., and Lam, A. K.-Y. (2018). Role of miR-193a in cancer: complexity and factors control the pattern of its expression. *Curr. Cancer Drug Targets* 18, 618–628. doi: 10.2174/1568009618666180308105727
- Mann, M., Wright, P. R., and Backofen, R. (2017). IntaRNA 2.0: enhanced and customizable prediction of RNA-RNA interactions. *Nucleic Acids Res.* 45, W435–W439. doi: 10.1093/nar/gkx279
- Mayrhofer, M., Gourain, V., Reischl, M., Affaticati, P., Jenett, A., Joly, J.-S., et al. (2017). A novel brain tumour model in zebrafish reveals the role of YAP activation in MAPK- and PI3K-induced malignant growth. *Dis. Model Mech.* 10, 15–28. doi: 10.1242/dmm.026500
- Nakano, H., Yamada, Y., Miyazawa, T., and Yoshida, T. (2013). Gain-of-function microRNA screens identify miR-193a regulating proliferation and apoptosis in epithelial ovarian cancer cells. *Int. J. Oncol.* 42, 1875–1882. doi: 10.3892/ijo.2013.1896
- Ory, B., Ramsey, M. R., Wilson, C., Vadysirisack, D. D., Forster, N., Rocco, J. W., et al. (2011). A microRNA-dependent program controls p53-independent survival and chemosensitivity in human and murine squamous cell carcinoma. *J. Clin. Invest.* 121, 809–820. doi: 10.1172/JCI43897
- Pase, L., and Lieschke, G. J. (2009). Validating microRNA target transcripts using zebrafish assays. *Methods Mol. Biol.* 546, 227–240. doi: 10.1007/978-1-60327-977-2_14
- Philippidou, D., Schmitt, M., Moser, D., Margue, C., Nazarov, P. V., Muller, A., et al. (2010). Signatures of microRNAs and selected microRNA target genes in human melanoma. *Cancer Res.* 70, 4163–4173. doi: 10.1158/0008-5472.CAN-09-4512
- Rahman, S., Sowa, M. E., Ottinger, M., Smith, J. A., Shi, Y., Harper, J. W., et al. (2011). The Brd4 extraterminal domain confers transcription activation independent of pTEFb by recruiting multiple proteins, including NSD3. *Mol. Cell. Biol.* 31, 2641–2652. doi: 10.1128/MCB.0134110
- Saba, R., Sorensen, D. L., and Booth, S. A. (2014). MicroRNA-146a: a dominant, negative regulator of the innate immune response. *Front. Immunol.* 5:578. doi: 10.3389/fimmu.2014.00578
- Santoriello, C., Deflorian, G., Pezzimenti, F., Kawakami, K., Lanfranccone, L., d'Adda di Fagagna, F., et al. (2009). Expression of H-RASV12 in a zebrafish model of Costello syndrome causes cellular senescence in adult proliferating cells. *Dis. Model Mech.* 2, 56–67. doi: 10.1242/dmm.001016
- Santoriello, C., Gennaro, E., Anelli, V., Distel, M., Kelly, A., Köster, R. W., et al. (2010). Kita driven expression of oncogenic HRAS leads to early onset and highly penetrant melanoma in zebrafish. *PLoS One* 5:e15170. doi: 10.1371/journal.pone.0015170
- Tibrewal, N., Liu, T., Li, H., and Birge, R. B. (2007). Characterization of the biochemical and biophysical properties of the phosphatidylserine receptor (PS-R) gene product. *Mol. Cell. Biochem.* 304, 119–125. doi: 10.1007/s11010-007-9492-8
- Uhlen, M., Zhang, C., Lee, S., Sjöstedt, E., Fagerberg, L., Bidkhori, G., et al. (2017). A pathology atlas of the human cancer transcriptome. *Science* 357:eaan2507. doi: 10.1126/science.aan2507
- Webby, C. J., Wolf, A., Gromak, N., Dreger, M., Kramer, H., Kessler, B., et al. (2009). Jmjd6 catalyses lysyl-hydroxylation of U2AF65, a protein associated with RNA splicing. *Science* 325, 90–93. doi: 10.1126/science.1175865
- Conflict of Interest Statement:** The authors declare that the research was conducted in the absence of any commercial or financial relationships that could be construed as a potential conflict of interest.

Copyright © 2018 Anelli, Ordas, Kneitz, Sagredo, Gourain, Scharlt, Meijer and Mione. This is an open-access article distributed under the terms of the Creative Commons Attribution License (CC BY). The use, distribution or reproduction in other forums is permitted, provided the original author(s) and the copyright owner(s) are credited and that the original publication in this journal is cited, in accordance with accepted academic practice. No use, distribution or reproduction is permitted which does not comply with these terms.